

Power Oscillation Damping Capabilities of Doubly Fed Wind Generators

Mohamed Edrah, Kwok L Lo, Abdussalam Elansari, Olimpo Anaya-Lara
University of Strathclyde, Glasgow, UK
mohamed.edrah@strath.ac.uk

Abstract—With the increased levels of wind power penetration into power systems, the influence of wind power on stability of power systems requires more investigation. Conventional synchronous generators are increasingly replaced by wind turbines and thus wind turbines have to contribute to power system stability. In this paper, the effects of double fed induction generator (DFIG) based wind farms and their controllers on small signal stability are investigated. Moreover, since wind turbines have to contribute to power system oscillation damping, a power oscillation damping controller within DFIG rotor side converter is developed in this study. The proposed damping control is validated on realistic Western System Coordinating Council (WSCC) power system consisting of DFIG based wind farm and synchronous generators. The simulation results show the effectiveness of the proposed power oscillation damping controller. With the proposed controller, DFIG based wind farm improves the system small signal stability dramatically by damping the system oscillations effectively.

Index Terms-- Doubly fed induction generator (DFIG), power oscillation damping, Power system stabilizer (PSS).

I. INTRODUCTION

In recent years, the integration of wind power into power systems has increased rapidly. During the last decade, the installed capacity of wind turbines has increased at an unexpected rate, and the wind turbines costs have also decreased [1]. Most of the recently installed wind turbines are variable speed wind turbines employing doubly fed induction generators. With the increased levels of DFIG, the influence of DFIG on small signal stability of power systems needs more attention.

As DFIGs are relatively new technologies in comparison with conventional synchronous generators, their dynamic behaviour are still under research. Recently, an increased research effort is devoted to address the stability of power systems with the increased penetration of wind power. The impact of wind power on power system oscillations was investigated in [2]. The results indicate that the penetration of wind power tend to improve the system oscillations and does not induce new oscillatory modes. Power electronic converter of the DFIG acts as an interface between DFIG generator and the grid. Therefore, with the increased penetration of DFIG wind farms, the effective inertia of the system will be reduced [3]. Since all of wind power generators are not synchronously coupled to the power systems, the turbine itself does not participate in

electromechanical oscillations. Rather, the penetration of wind power will have a damping effect due to reduction in the size of synchronous generators that engaged in power system oscillations. However, the effect of wind power generators on small signal stability depends on the kind of wind generator and their controllers [4].

To improve the oscillations damping of power systems with high penetration of DFIG based wind farms, an auxiliary damping control loop for DFIG is used. Eigenvalue analysis and time domain simulation was used in [5] to study the capability of DFIG to damp power oscillations. The results indicate that damping of network oscillation can be significantly enhanced by a proper designed DFIG power system stabilizer (PSS). The proposed PSS can work over full operation slip without degradation the system voltage. In the above study, the adopted PSS is similar to the PSS of the synchronous generators and it was attached to the active power control loop of the DFIG rotor side converter (RSC). In [6], a two area system with a large wind farm is analysed by a time domain simulator. An auxiliary damping control loop is added to the DFIG-RSC to improve the damping of inter-area oscillations in high wind power penetration. The paper concluded that the active power modulation of DFIG based wind farm is an effective method for damping oscillations in power systems. Moreover, reference [7] stated that DFIG is able to improve power oscillations better than other types of wind generators even in weak systems. DFIG based wind farms are capable to control active and reactive power independently that both could be used to improve small signal stability. Vector control technique can be used to achieve this decoupled control strategy.

In this paper, the effect of DFIG based wind farms on power system small signal stability and their control capabilities to enhance the damping of network oscillations are investigated. A supplementary damping control is proposed within RSC of DFIG wind farm. Moreover, as the new wind farms have to contribute to the grid voltage regulation, the effect of DFIG voltage control mode on the proposed damping control is considered.

This paper is organised as follows: First, the modelling of DFIG is described Section II. Then a simple real test system is described in Section III. After that the results and discussion of a number of cases are outlined in section IV. Finally, the paper conclusions are summarised in section V.

II. MODELLING OF DFIG

The general structure of DFIG based wind turbine is shown in Fig. 1. The DFIG consists of wind turbine, gear box, a wound rotor induction generator, back-to-back converter and their controllers. The induction generator stator is directly connected to the grid whereas the rotor is fed through the back-to-back voltage source converter. The crowbar is used, during grid faults, to protect the rotor side converter from over current in the rotor circuit.

The DFIG based wind farm is modelled in details in the simulation tool. However, as the main purpose of this study is to examine the impact of DFIG on power system small signal stability and analyses the capability of DFIG based wind farm to damp power systems oscillations, only the modelling of induction generator and DFIG-RSC is mentioned in the text.

A. Generator Modelling

The induction generator stator and rotor differential equations can be expressed as follows:

$$\mathbf{v}_{sabc} = R_s \mathbf{i}_{sabc} + \frac{d\psi_{sabc}}{dt} \quad (1)$$

$$\mathbf{v}_{rabc} = R_r \mathbf{i}_{rabc} + \frac{d\psi_{rabc}}{dt} \quad (2)$$

Applying synchronous reference frame transformation rotating by angular speed ω_s to the above equations, the differential equations of the DFIG induction machine in $d-q$ are [8, 9]:

$$\mathbf{v}_{ds} = R_s \mathbf{i}_{ds} - \omega_s \psi_{qs} + \frac{d\psi_{ds}}{dt} \quad (3)$$

$$\mathbf{v}_{qs} = R_s \mathbf{i}_{qs} + \omega_s \psi_{ds} + \frac{d\psi_{qs}}{dt} \quad (4)$$

$$\mathbf{v}_{dr} = R_r \mathbf{i}_{dr} - (\omega_s - \omega_r) \psi_{qr} + \frac{d\psi_{dr}}{dt} \quad (5)$$

$$\mathbf{v}_{qr} = R_r \mathbf{i}_{qr} + (\omega_s - \omega_r) \psi_{dr} + \frac{d\psi_{qr}}{dt} \quad (6)$$

Where $\mathbf{v}_{qs}, \mathbf{i}_{qs}, \psi_{qs}$ are respectively the stator voltage, current and flux linkage in the q axis, and $\mathbf{v}_{qr}, \mathbf{i}_{qr}, \psi_{qr}$ are respectively the rotor voltage, current and flux linkage in the q axis. $\mathbf{v}_{ds}, \mathbf{i}_{ds}, \psi_{ds}$ are respectively the stator voltage, current and flux linkage in the d axis, and likewise $\mathbf{v}_{dr}, \mathbf{i}_{dr}, \psi_{dr}$ are respectively the rotor voltage, current and flux linkage in the d axis. ω_s and ω_r are rotational speed of the synchronous reference frame and the rotor speed.

Flux linkage equations in $d-q$ axis:

$$\psi_{ds} = L_{ls} \mathbf{i}_{ds} + L_m (\mathbf{i}_{ds} + \mathbf{i}_{dr}) = L_s \mathbf{i}_{ds} + L_m \mathbf{i}_{dr} \quad (7)$$

$$\psi_{qs} = L_{ls} \mathbf{i}_{qs} + L_m (\mathbf{i}_{qs} + \mathbf{i}_{qr}) = L_s \mathbf{i}_{qs} + L_m \mathbf{i}_{qr} \quad (8)$$

$$\psi_{dr} = L_{lr} \mathbf{i}_{dr} + L_m (\mathbf{i}_{ds} + \mathbf{i}_{dr}) = L_r \mathbf{i}_{dr} + L_m \mathbf{i}_{ds} \quad (9)$$

$$\psi_{qr} = L_{lr} \mathbf{i}_{qr} + L_m (\mathbf{i}_{qs} + \mathbf{i}_{qr}) = L_r \mathbf{i}_{qr} + L_m \mathbf{i}_{qs} \quad (10)$$

Where the stator L_s and rotor L_r inductance are defined by:

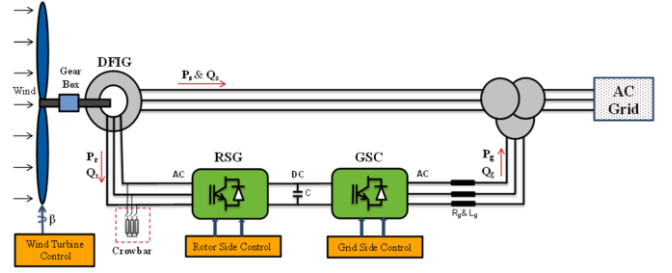


Fig. 1. General structure of DFIG wind turbine with controls.

$$L_s = L_{ls} + L_m, \quad L_r = L_{lr} + L_m \quad (11)$$

In which L_m is the mutual inductance and L_{ls}, L_{lr} are the stator and rotor leakage inductance.

Neglecting the stator and rotor power losses, the equations of active and reactive power are:

$$P_s = \frac{3}{2} (\mathbf{v}_{ds} \mathbf{i}_{ds} + \mathbf{v}_{qs} \mathbf{i}_{qs}), \quad Q_s = \frac{3}{2} (\mathbf{v}_{qs} \mathbf{i}_{ds} - \mathbf{v}_{ds} \mathbf{i}_{qs}) \quad (12)$$

$$P_r = \frac{3}{2} (\mathbf{v}_{dr} \mathbf{i}_{dr} + \mathbf{v}_{qr} \mathbf{i}_{qr}), \quad Q_r = \frac{3}{2} (\mathbf{v}_{qr} \mathbf{i}_{dr} - \mathbf{v}_{dr} \mathbf{i}_{qr}) \quad (13)$$

The torque in $d-q$ axis is given by the following equation:

$$T_e = \psi_{ds} \mathbf{i}_{qs} - \psi_{qs} \mathbf{i}_{ds} = \psi_{qr} \mathbf{i}_{dr} - \psi_{dr} \mathbf{i}_{qr} = L_m (\mathbf{i}_{qs} \mathbf{i}_{dr} - \mathbf{i}_{ds} \mathbf{i}_{qr}) \quad (14)$$

Where T_e is the electromagnetic torque developed by the induction generator.

B. Rotor Side Converter Modelling

The control of DFIG stator active power P_s and reactive power Q_s is achieved by controlling the rotor current \mathbf{i}_{rabc} in the stator flux oriented reference frame [10]. The rotor current \mathbf{i}_{rabc} are transferred to $d-q$ current component \mathbf{i}_{dr} and \mathbf{i}_{qr} in the stator flux oriented reference frame.

In the stator flux oriented reference frame, the ψ_s (stator flux linkage) is aligned to the d axis. Therefore, the stator flux linkage in $d-q$ will be $(\psi_s = \psi_{ds})$ and $(\psi_{qs} = 0)$ [8].

$$\text{From equation (8)} \quad \mathbf{i}_{qs} = -\frac{L_m}{L_s} \mathbf{i}_{qr} \quad (15)$$

From equation (3), (4) and (7)

$$\mathbf{i}_{ds} = \frac{L_m}{L_s} \left(\frac{\mathbf{v}_{qs} - R_s \mathbf{i}_{qs}}{\omega_s L_m} - \mathbf{i}_{dr} \right) = \frac{L_m}{L_s} (\mathbf{i}_{ms} - \mathbf{i}_{dr}) \quad (16)$$

$$\text{Where: } \mathbf{i}_{ms} = \frac{\mathbf{v}_{qs} - R_s \mathbf{i}_{qs}}{\omega_s L_m} \quad (17)$$

In this case equation (12) can be rewritten as:

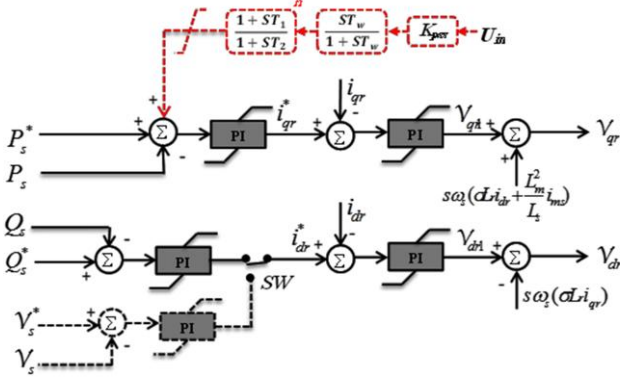


Fig. 2. Overall vector control scheme of the DFIG rotor side converter, voltage control strategy (dashed black lines), proposed damping control attached to active power control loop (dashed red lines).

$$P_s = -\frac{3}{2}(\omega_s \frac{L_m^2}{L_s} i_{ms} i_{qr}), \quad Q_s = \frac{3}{2}(\omega_s \frac{L_m^2}{L_s} i_{ms} (i_{ms} - i_{dr})) \quad (18)$$

By substituting equations (9), (10), (15) and (16) into (5), (6)

$$v_{dr} = R_r i_{dr} + \sigma L_r \frac{d}{dt} i_{dr} - (\omega_s - \omega_r) \sigma L_r i_{qr} \quad (19)$$

$$v_{qr} = R_r i_{qr} + \sigma L_r \frac{d}{dt} i_{qr} + (\omega_s - \omega_r) [\sigma L_r i_{dr} + \frac{L_m^2}{L_s} i_{ms}] \quad (20)$$

$$\text{Where } \sigma = 1 - \frac{L_m^2}{L_s L_r} \quad (21)$$

Equation (18) shows that DFIG stator active and reactive power (P_s and Q_s) can be controlled independently by the d - q axes rotor current i_{qr} and i_{dr} respectively. The reference values of rotor current i_{qr} and i_{dr} can be determined directly from P_s and Q_s by the outer power control loops.

By rewriting the equations (19), (20)

$$v_{dr} = v_{dr1} - v_{dr2} \quad (22)$$

$$v_{qr} = v_{qr1} + v_{qr2} \quad (23)$$

Where

$$v_{dr1} = R_r i_{dr} + \sigma L_r \frac{d}{dt} i_{dr} \quad (24)$$

$$v_{qr1} = R_r i_{qr} + \sigma L_r \frac{d}{dt} i_{qr} \quad (25)$$

$$v_{dr2} = (\omega_s - \omega_r) \sigma L_r i_{qr} \quad (26)$$

$$v_{qr2} = (\omega_s - \omega_r) [\sigma L_r i_{dr} + \frac{L_m^2}{L_s} i_{ms}] \quad (27)$$

The rotor current i_{dr} and i_{qr} of equations (24) and (25) in term of v_{dr1} and v_{qr1} can be written as:

$$\frac{d}{dt} i_{dr} = -\frac{R_r i_{dr}}{\sigma L_r} + \frac{1}{\sigma L_r} v_{dr1} \quad (28)$$

$$\frac{d}{dt} i_{qr} = -\frac{R_r i_{qr}}{\sigma L_r} + \frac{1}{\sigma L_r} v_{qr1} \quad (29)$$

Equations (28) and (29) indicate that i_{dr} and i_{qr} respond to v_{dr1} and v_{qr1} respectively. Therefore, a proportional-integral (PI) controller can be designed as follows:

$$v_{dr1} = (k_{pr} + \frac{k_{ir}}{s})(i_{dr}^* - i_{dr}) \quad (30)$$

$$v_{qr1} = (k_{pr} + \frac{k_{ir}}{s})(i_{qr}^* - i_{qr}) \quad (31)$$

Substituting equations (30) and (31) into (22) and (23)

$$v_{dr} = (k_{pr} + \frac{k_{ir}}{s})(i_{dr}^* - i_{dr}) - s \omega_s (\sigma L_r i_{qr}) \quad (32)$$

$$v_{qr} = (k_{pr} + \frac{k_{ir}}{s})(i_{qr}^* - i_{qr}) + s \omega_s (\sigma L_r i_{dr} + \frac{L_m^2}{L_s} i_{ms}) \quad (33)$$

Fig. 2 shows the overall vector control scheme of the DFIG-RSC. The reference signals i_{dr}^* and i_{qr}^* in the outer control loops are generated by controlling the stator reactive and active power respectively. Then, the error signals are generated by deducting the current signals i_{dr} and i_{qr} from reference signals i_{dr}^* and i_{qr}^* respectively. The generated error signals are formed into two voltage signals v_{dr1} and v_{qr1} by the inner control loops using two PI controllers. Finally, the output of the inner current loops (v_{dr1} and v_{qr1}) are compensated by the corresponding cross coupling terms (v_{dr2} and v_{qr2}) to form the d - q voltage signals (v_{dr} and v_{qr}) respectively. These signals are then connected to Pulse width modulation (PWM) to create signals for the IGBT gate control [11], [12].

C. Damping Control Modelling

As explained in rotor side converter modelling, the active and reactive power (P_s and Q_s) of DFIG can be controlled independently by controlling the rotor current i_{qr} and i_{dr} respectively. These control loops can be used to improve the power system stability by adding additional signals. Therefore, a robust control strategy could improve the damping of power system oscillations by adding an additional signal to the active or reactive power control loops. In this paper, the additional signal is attached to the active power control loop of DFIG. The signal of damping control is added to the reference power (P_s^*). The reference power is calculated by using the maximum power point tracking (MPPT) lookup table. The DFIG-RSC with the auxiliary damping control is shown in Fig. 2.

The main purpose of the damping control is to increase the damping of poorly damped oscillations. These oscillations are in low frequency range of 0.1 to 2 Hz. Any measured signal that is affected by the oscillations can be employed as an input signal by the damping control. Local signals are preferred to avoid communication issues and delays. In this work, the frequency deviation at the terminal of wind farm is chosen as an input signal to the proposed damping control.

The input signal is provided with a constant gain to determine the amount of damping and filtered by a washout block to eliminate any steady state variation. Then the signal is passed through a lead-lag compensator to provide the required phase shift. The proposed oscillation damping control is similar to the conventional PSS and it is represented by equation (34) [23].

$$u_{pss} = K_{pss} \left(\frac{ST_w}{1+ST_w} \right) \left(\frac{1+ST_1}{1+ST_2} \right)^n u_{in} \quad (34)$$

Where, u_{in} and u_{pss} are control input and output signals respectively, K_{pss} is the controller gain, T_w is a washout time constant (s) and T_1 to T_2 are lead-lag time constants (s).

III. TEST SYSTEM

In order to study the effect of DFIG wind turbines on power system small signal stability and their oscillation damping capability, a nine buses test system is used as shown in Fig. 3. The system total load is 315 MW and 115 MVar. The three synchronous generators are equipped with an automatic voltage regulator of IEEE type 1. However, for more straightforward assessment, none of the three synchronous generators are equipped with power system stabilizer. Generators G_1 and G_2 are equipped with turbine governor type TGOV1. The static and dynamic data of the test system can be found in [13].

A time domain simulation with a detailed model of synchronous generators and DFIG based wind farm is used in this study. The test system and the DFIG wind turbine are modelled and simulated by using NEPLAN software [14]. The three loads were modelled as 33% constant current, 33% constant power and 33% constant impedance [15].

The wind farm consists of 17 wind turbines aggregated into a large DFIG wind turbine. The DFIG based wind farm generates 85 MW which is similar amount to that generated from the replaced synchronous machine G_3 . In this case, the penetration level of wind power is about 27 % of the total load. The aggregation method used to aggregate the wind turbines in this study is explained in [16].

IV. RESULTS AND DISCUSSION

In this study, five different cases are analysed by eigenvalue and transient analysis to show the influence of DFIG on power systems small signal stability and to investigate the power oscillation damping capability of DFIG based wind farms. The description of each case is as following:

- **Case A:** there is no wind power connected to the test system. It is a base case in which the all generators are conventional synchronous generators.
- **Case B:** synchronous generator G_3 is replaced by a DFIG based wind farm with an equivalent rating. The wind farm

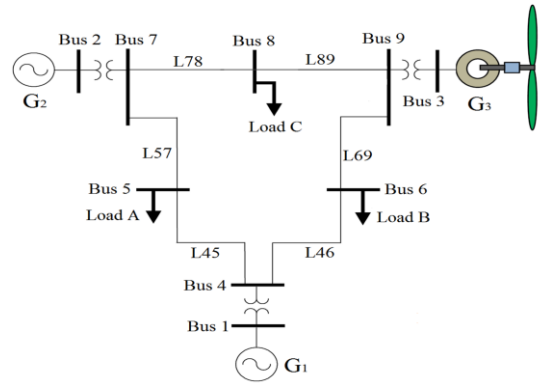


Fig. 3. Single line diagram of the test system with DFIG based wind farm.

is operating at a unity power factor (no reactive power is exchanged between the test system and the wind farm).

- **Case C:** The wind farm is operating on voltage control mode in which the terminal voltage is controlled at 1 pu (the reactive power of DFIG stator is used to control the wind farm terminal voltage).
- **Case D:** The wind farm is operating at a unity power factor and it is equipped with the proposed damping control.
- **Case E:** The wind farm is operating on voltage control mode controlling its terminal voltage at 1 pu and it is equipped with the proposed damping control.

A. Eigenvalue Analysis

The electromechanical oscillations of the test system in the frequency range of 0.1 to 2 Hz are observed. The dominant modes for the first three cases case can be seen in Table I.

TABLE I
DOMINANT EIGENVALUE OF CASES A- C

Cases	A	B	C
Eigenvalue	-0.282 ±j6.919	-0.314±j7.067	-0.316 ± 7.081
$\lambda = \sigma + j\omega$ (pu)			
Frequency f (Hz)	1.101	1.125	1.127
Damping Factor ζ (%)	4.1	4.4	4.5
Dominant variable	ρ, ω	ρ, ω	ρ, ω
Dominant Machine	G_2	G_2	G_2
Participation factor (%)	35.3, 37.6	39.9, 42.5	40.1, 42.5

The three main modes are oscillating at a near similar frequency. However, replacing a synchronous generator with an equivalent DFIG wind farm improves the damping of electromechanical oscillations. The dominant eigenvalue damping factor is increased to 4.4 % in the case of wind farm. Furthermore, the damping of the oscillation is improved further to 4.5 % when the wind farm controlling its terminal voltage. In addition, contribution of G_2 to the oscillatory mode in cases B & C is higher than the first scenario. This is because DFIG wind farm has no contribution to the oscillatory modes.

In the synchronous generators case, the dominant oscillation gets the contribution from the three synchronous generators. The first generator is swinging against the other two. However, in the case of wind farm, there is no contribution from the DFIG. In this case, oscillation gets the contribution from G_1 and G_2 which are oscillating against each other.

To investigate the oscillation damping capability of DFIG wind farm, a supplementary damping control is used, within the active power control loop of the wind farm, in the last two cases. As can be seen in Table II, the proposed PSS has shifted the dominant eigenvalues toward the stable region in both cases. The damping factor is increased from 4.4 % (case B) to 7.6 % (case D) respectively. This indicates that the proposed damping control is effectively enhancing the damping of the oscillatory main mode. In a similar way, the damping is increased from 4.5 % (case C) to 7.4 % (case E). However, this amount of damping is less than that in case D.

Cases	D	E
Eigenvalue	-0.55 ±j7.206	-0.536±j7.195
$\lambda = \sigma + j\omega$ (pu)		
Frequency f (Hz)	1.147	1.145
Damping Factor ζ (%)	7.6	7.4
Dominant variable	ρ, ω	ρ, ω
Dominant Machine	G_2	G_2
Participation factor (%)	41.6, 44.2	41.7, 44.3

It is worth to note that replacing a synchronous generator with an equivalent DFIG based wind farm improves slightly the small signal stability of the power system. The damping of the oscillatory eigenvalues can be enhanced further when the terminal voltage of the wind farm controlled. However, controlling the terminal voltage of wind farms that are equipped with PSS can reduce their damping capability.

B. Transient Analysis

In this section, the effectiveness of the proposed damping control is examined during system transient by a time domain simulator. In this case, the test system is exposed to a large disturbance, three-phase short circuit fault. The fault is chosen to be close to G_2 the most critical generator. Therefore, a three-phase to ground fault for 150 ms was imposed near bus 7. The fault was cleared by opening the faulted line (line 5-7) from both sides simultaneously.

The dynamic response of G_2 rotor angles relevant to G_1 during transient period are plotted together for all the cases as shown in Fig. 4. It is clear that the proposed damping control damps the oscillation effectively. The rotor angle variations in the case of damping control are damped in just 6 s. However, the rotor angle variations in the case of synchronous generator and wind farm without damping control continue to oscillate after 10 s. Moreover, the rotor angles oscillations show that DFIG with PSS and operated at

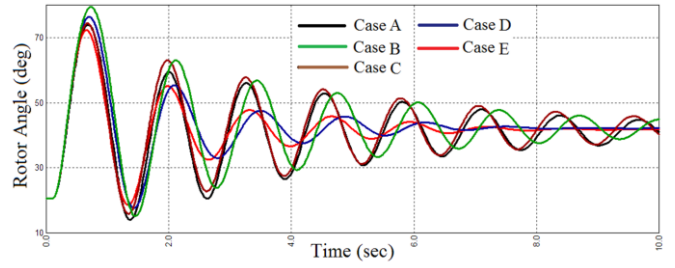


Fig. 4. Relative rotor angle of G_2 for each case.

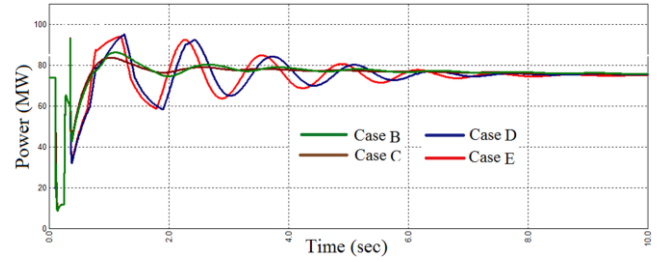


Fig. 5. Transient responses of the wind farm active power for each case.

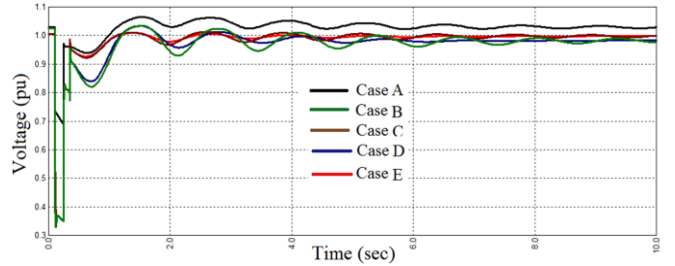


Fig. 6. Transient responses of G_3 and the wind farm terminal voltage for each case.

a unity power factor can damp the oscillation more effectively than a wind farm with PSS and terminal voltage control.

Fig. 5 shows the DFIG active power without and with damping control. The active power after the disturbance, in the case of damping control, is more fluctuant than that in the case without damping control. This variation in active power is a result of damping control that is included in the active power control loop of DFIG. However, with the sufficient damping of the proposed damping control the fluctuation disappears quickly.

Fig. 6 shows the dynamic responses of the wind farm terminal voltage for each case. From Fig. 6, the wind farm terminal voltage reaches to near 0.8 pu after the fault is cleared but the crowbar is still active. At this time the induction generator absorbs a large amount of reactive power. Moreover, it is clear that the terminal voltage of the wind farm in the case of the unity power factor control recovers slowly and continues to oscillate until the electromechanical oscillation disappears. However, in the case of voltage control mode, the terminal voltage is relatively smooth.

V. CONCLUSIONS

In this paper, the influence of DFIG based wind farms and their controllers on power system small signal stability are investigated. Moreover, a power oscillation damping controller is proposed and examined in this study. From the results of this study, the DFIG based wind farms have no negative impact on power system small signal stability, because wind generators have no contribution to the system electromechanical oscillations. However, DFIG based wind farms have the capability to improve power oscillations. The inclusions of the proposed damping control within RSC of the DFIG wind farm can substantially improve the damping of the oscillation. The effectiveness of the proposed control is also demonstrated by a time domain simulation. Furthermore, the results also indicate that the effectiveness of the damping control can be reduced if DFIG reactive power is used to control the terminal voltage of wind farm.

REFERENCES

- [1] T. Ackermann, *Wind Power in Power Systems*: John Wiley & Sons, Ltd, 2005.
- [2] J. Slootweg and W. Kling, "The impact of large scale wind power generation on power system oscillations," *Electric Power Systems Research*, vol. 67, pp. 9-20, 2003.
- [3] M. V. A. Nunes, J. A. Peas Lopes, H. H. Zurn, U. H. Bezerra, and R. G. Almeida, "Influence of the variable-speed wind generators in transient stability margin of the conventional generators integrated in electrical grids," *Energy Conversion, IEEE Transactions on*, vol. 19, pp. 692-701, 2004.
- [4] Y. Sun, L. Wang, G. Li, and J. Lin, "A review on analysis and control of small signal stability of power systems with large scale integration of wind power," in *Power System Technology (POWERCON), 2010 International Conference on*, 2010, pp. 1-6.
- [5] F. M. Hughes, O. Anaya-Lara, N. Jenkins, and G. Strbac, "A power system stabilizer for DFIG-based wind generation," *Power Systems, IEEE Transactions on*, vol. 21, pp. 763-772, 2006.
- [6] Z. Miao, L. Fan, D. Osborn, and S. Yuvarajan, "Control of DFIG-based wind generation to improve interarea oscillation damping," *Energy Conversion, IEEE Transactions on*, vol. 24, pp. 415-422, 2009.
- [7] H. Huazhang and C. Y. Chung, "Design of a Power Oscillation Damper for DFIG-based Wind Energy Conversion System Using Modified Particle Swarm Optimizer," in *Modelling Symposium (AMS), 2012 Sixth Asia*, 2012, pp. 161-166.
- [8] Q. Wei, "Dynamic modeling and control of doubly fed induction generators driven by wind turbines," in *Power Systems Conference and Exposition, 2009. PSCE '09. IEEE/PES*, 2009, pp. 1-8.
- [9] J. Zhenhua and Y. Xunwei, "Modeling and control of an integrated wind power generation and energy storage system," in *Power & Energy Society General Meeting, 2009. PES '09. IEEE*, 2009, pp. 1-8.
- [10] Q. Liyan and Q. Wei, "Constant Power Control of DFIG Wind Turbines With Supercapacitor Energy Storage," *Industry Applications, IEEE Transactions on*, vol. 47, pp. 359-367, 2011.
- [11] Q. Wei, G. K. Venayagamoorthy, and R. G. Harley, "Real-Time Implementation of a STATCOM on a Wind Farm Equipped With Doubly Fed Induction Generators," *Industry Applications, IEEE Transactions on*, vol. 45, pp. 98-107, 2009.
- [12] L. Qu and W. Qiao, "Constant power control of DFIG wind turbines with supercapacitor energy storage," *Industry Applications, IEEE Transactions on*, vol. 47, pp. 359-367, 2011.
- [13] P. M. Anderson and A. A. Fouad, *POWER SYSTEM CONTROL AND STABILITY*: Wiley-IEEE Press 2003.
- [14] B. B. C. P. Inc. "NEPLAN® Power System Analysis and Engineering", . Available: http://www.neplan.ch/html/e/e_home.htm
- [15] "Standard load models for power flow and dynamic performance simulation," *Power Systems, IEEE Transactions on*, vol. 10, pp. 1302-1313, 1995.
- [16] L. M. Fernandez, C. A. Garcia, J. R. Saenz, and F. Jurado, "Reduced model of DFIGs wind farms using aggregation of wind turbines and equivalent wind," in *Electrotechnical Conference, 2006. MELECON 2006. IEEE Mediterranean*, 2006, pp. 881-884.